RIS-Assisted Joint Sensing and Communications via Fractionally Constrained Fractional Programming

Yiming Liu and Wei Yu
Department of Electrical & Computer Engineering, University of Toronto, Toronto, Canada
E-mails: eceym.liu@mail.utoronto.ca, weiyu@ece.utoronto.ca

***Abstract*—This paper studies an uplink dual-functional sensing and communication system assisted by an active or passive reconfigurable intelligent surface (RIS), whose reflection pattern is optimally configured to trade off sensing and communication functionalities. Specifically, the Bayesian Cramér-Rao lower bound (BCRLB) for sensing is minimized under the quality-of-service (QoS) communication constraints. We show that this problem can be formulated as a fractionally constrained fractional programming (FCFP) problem for which a quadratic transform, originally proposed for the sum-of-ratio fractional programs, can be used to decouple the numerators and denominators in both the objective function and the constraints. In this way, the FCFP is turned into a sequence of sub-problems that are convex except for the constant-modulus amplitude constraints which can be dealt with using a penalty-based method. Numerical results unveil nontrivial beamforming reflection patterns that the RIS can be configured to generate in order to facilitate both sensing and communications. The results demonstrate the effectiveness of the proposed algorithm.**

I. Introduction

With the increasing demands on location information and for sensing functionality in the beyond-fifth-generation (5G) and six-generation (6G) wireless networks, integrated sensing and communications is seen as a promising use case for future networks [1]. Reconfigurable intelligent surface (RIS) is a viable and promising solution to achieve this purpose [2]–[5], especially in practical scenarios with many obstructions. This paper investigates the optimal configuration of an active or passive RIS to trade off sensing and communication functionalities for systems such as the one shown in Fig. 1, where the direct paths between the users and the base station (BS) are blocked and the reflection pattern of the RIS needs to be optimally configured in order to serve both the sensing and communication purposes.

There are many prior works investigating RIS-aided wireless sensing [5]–[11], where the Cramér-Rao lower bound (CRLB) is often used as the performance metric for sensing. However, the CRLB is not easy to optimize, especially in a system involving RIS and especially when both communication and sensing functionalities are involved. For example, [10] adopts the CRLB to evaluate the target estimation performance in a system without RIS. In [11], the CRLB of an RIS-aided wireless sensing system is being minimized, however, the communication functions are not integrated into the system. Moreover, it is important to note that CRLB depends on the exact values of the parameters to be estimated. In practice, however, only a prior distribution of the parameters to be sensed is known. Therefore, Bayesian CRLB (BCRLB) (e.g., [12]) is more suitable to be adopted as a sensing metric.

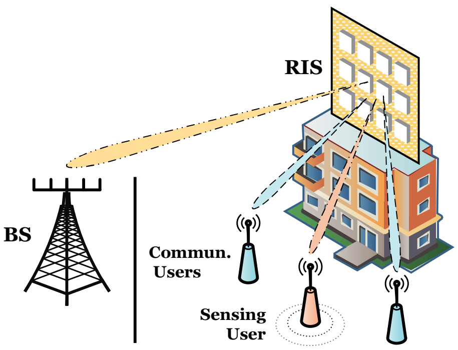

Fig. 1. An RIS-assisted dual-functional sensing and communication system.

In this paper, we investigate an RIS-assisted dual-functional uplink sensing and communication system, where the RIS is considered as either active or passive, and the beamforming at the RIS is designed to trade off between the two functions. We tackle a specific problem of minimizing the BCRLB of an azimuth angle estimation problem for one sensing user under the quality-of-service (QoS) constraints for the communication users. We show that this novel problem formulation is a fractionally constrained fractional programming (FCFP) problem with extra RIS amplitude constraints. In order to address this challenging problem, we first extend a quadratic transform technique previously proposed to handle optimization problems for which objective functions contain fractional structures [13] to the scenario under consideration where the constraints also contain fractional structures. This allows the FCFP problem to be transformed into a sequence of sub-problems which are convex except for the extra constant-modulus amplitude constraints in the passive RIS case. Finally, a penalty-based method is used to deal with the constant-modulus constraints. Numerical results demonstrate the effectiveness of the proposed algorithm and show that the optimization can produce nontrivial RIS reflection patterns that facilitate both sensing and communication functionalities at the same time.

II. System Model

Consider an uplink RIS-assisted dual-functional sensing and communication system where an M-antenna base station (BS) intends to estimate the azimuth angle η_0 from one single-antenna sensing user to an $N \times N$ RIS, while providing uplink communication service for K single-antenna users, as illustrated in Fig. 1. We use index 0 to represent the sensing user and indices 1 to K to represent the communication users. The azimuth angle of arrival from the k-th user to the RIS is represented by η_k. For simplicity, we model the RIS as a planar array. The reflecting operation at the N^2 elements can be modeled as

$$\begin{aligned}\mathbf{\Phi} &= \mathrm{diag}\left(\mathbf{x}^{\mathsf{T}}\right)\\ &\triangleq \mathrm{diag}\left(\left[\alpha_1 \exp\left(j\theta_1\right), \cdots, \alpha_{N^2}\exp\left(j\theta_{N^2}\right)\right]\right),\end{aligned} \tag{1}$$

where $\theta_n \in [-\pi, \pi)$ is the phase shift of the n-th element, α_n is the corresponding amplitude, and $\mathbf{x}$ is the RIS beamforming vector to be optimized. This paper considers both passive and active RIS, for which the amplitudes of the elements of $\mathbf{x}$ are constrained as [3]

$$|x_n| \le \alpha_{\max},\ \forall n,\ \text{ if the RIS is active,} \tag{2}$$

$$|x_n| = 1,\qquad \forall n,\ \text{ if the RIS is passive,} \tag{3}$$

where $\alpha_{\max}$ is a predetermined maximum amplitude that the active RIS can provide.

We assume that the direct channels between the users and the BS are obstructed so that the radio propagation paths can only be established by the reflecting channels. We also assume that the RIS-BS channel, denoted as $\mathbf{G}$, follows the Rician fading model. Since this channel is shared by all sensing and communication users, it is assumed to be known at the BS. As the RIS is typically deployed in proximity to the users, in this paper we make the simplifying assumption that the user-RIS channel has only a line-of-sight component [14], and the channel $\mathbf{h}_k$ from the k-th user to the RIS can be determined by the steering vector $\mathbf{v}(\eta_k)$ as follows:

$$\mathbf{h}_k = \rho_k \mathbf{v}(\eta_k) \triangleq \rho_k \exp\left(j\tau\cos(\eta_k)\left[v(1), \cdots, v(N^2)\right]^{\mathsf{T}}\right), \tag{4}$$

where $\tau = 2\pi d/\omega$, ω is the carrier wavelength, d represents the spacing between the reflecting elements (typically at half wavelength), $v(n) = \mathrm{mod}\,(n-1, N)$, and ρ_k represents the fading coefficient, which is assumed to be known for now for simplicity, but in practice can be estimated or tracked using various techniques, e.g., see [15] and references herein.

Based on the channel model established above, the received signal at the BS can then be expressed as

$$\begin{aligned}\mathbf{y} &= \left(\mathbf{G}\mathbf{\Phi}\mathbf{h}_0\right)s_0 + \sum_{k=1}^{K}\left(\mathbf{G}\mathbf{\Phi}\mathbf{h}_k\right)s_k + \mathbf{n} \qquad (5)\\ &= \sum_{k=0}^{K} s_k\left[\mathbf{G}\,\mathrm{diag}(\mathbf{h}_k)\right]\mathrm{diag}^{-1}(\mathbf{\Phi}) + \mathbf{n} \triangleq \sum_{k=0}^{K} s_k \mathbf{H}_k\mathbf{x} + \mathbf{n},\end{aligned}$$

where s_0 denotes the pilot transmitted by the sensing user, $s_1, s_2, \cdots, s_K$ are the uplink data symbols transmitted by the K communication users, and $\mathbf{n}$ is the additive white Gaussian noise distributed as $\mathcal{CN}(\mathbf{0}, \sigma^2\mathbf{I})$. Here, the transmit signals $s_k, k = 0, \cdots, K$ are independent and distributed as $\mathcal{CN}(0, p_k)$ with transmit power p_k. We rely on beamforming to spatially separate the users, and assume no interference cancellation is performed.

III. Problem Formulation

A. Sensing Performance Metric

CRLB, which is a lower bound on the mean squared error of an unbiased estimator, is widely adopted for characterizing sensing performance. Since in this paper, we only consider the estimation of one single azimuth angle, the CRLB is simply the inverse of the scalar Fisher information, given by

$$\mathrm{J}(\mathbf{y};\eta_0) = 2p_0\left(\dot{\mathbf{H}}_0\mathbf{x}\right)^{\mathsf{H}}\mathbf{\Sigma}_0^{-1}(\mathbf{x})\left(\dot{\mathbf{H}}_0\mathbf{x}\right), \tag{6}$$

where $\dot{\mathbf{H}}_0 = \mathbf{G}\,\mathrm{diag}(\dot{\mathbf{h}}_0)$, and $\dot{\mathbf{h}}_0$ is the derivative of $\mathbf{h}_0$ with respect to η_0. The n-th entry of $\dot{\mathbf{h}}_0$ can be computed as

$$\left[\dot{\mathbf{h}}_0\right]_n = -j\rho_k\tau\sin(\eta_0)\,v(n)\exp\left[j\tau\cos(\eta_0)\,v(n)\right]. \tag{7}$$

The Fisher information contains a covariance matrix term $\mathbf{\Sigma}_0(\mathbf{x})$, as a function of the optimization variable $\mathbf{x}$, given by

$$\mathbf{\Sigma}_0(\mathbf{x}) = \sum_{k=1}^{K} p_k\left(\mathbf{H}_k\mathbf{x}\right)\left(\mathbf{H}_k\mathbf{x}\right)^{\mathsf{H}} + \sigma^2\mathbf{I}. \tag{8}$$

Note that this classic CRLB depends on the true azimuth angle η_0 of the sensing user as in (7), which in practice is unknown and needs to be estimated. Thus, we cannot directly utilize the classic CRLB to evaluate the sensing performance. To this end, we adopt the Bayesian version of the CRLB, accounting for the prior distribution of η_0, based on the historical observations and/or prior knowledge.

Denote the probability density function (PDF) of the prior distribution of η_0 as $p(\eta_0)$. The BCRLB can be expressed as

$$\mathcal{B}(\eta_0) = \left(\mathbb{E}_{\eta_0}[\mathrm{J}(\mathbf{y};\eta_0)] + \mathrm{J}_o(\eta_0)\right)^{-1}, \tag{9}$$

where $\mathrm{J}(\mathbf{y};\eta_0)$ is the Fisher information given in (6), and the expectation of $\mathrm{J}(\mathbf{y};\eta_0)$ is taken with respect to $p(\eta_0)$, and $\mathrm{J}_o(\eta_0)$ is the Fisher information of the prior distribution of η_0 and is independent of the optimization variable $\mathbf{x}$. Consequently, minimizing $\mathcal{B}(\eta_0)$ with respect to $\mathbf{x}$ is equivalent to maximizing the expectation $\mathbb{E}_{\eta_0}[\mathrm{J}(\mathbf{y};\eta_0)]$ given by

$$\mathbb{E}_{\eta_0}[\mathrm{J}(\mathbf{y};\eta_0)] = 2p_0\int\left(\dot{\mathbf{H}}_0\mathbf{x}\right)^{\mathsf{H}}\mathbf{\Sigma}_0^{-1}(\mathbf{x})\left(\dot{\mathbf{H}}_0\mathbf{x}\right)p(\eta_0)\,d\eta_0. \tag{10}$$

The above expectation involves an integral and is complicated to evaluate and to optimize. The following theorem allows us to extract the optimization variable $\mathbf{x}$ from the integral.

Theorem 1: Consider a second moment matrix $\dot{\mathbf{U}}$ defined as

$$\dot{\mathbf{U}} \triangleq \mathbb{E}_{\eta_0}\left[\mathrm{vec}\left(\dot{\mathbf{H}}_0\right)\mathrm{vec}^{\mathsf{H}}\left(\dot{\mathbf{H}}_0\right)\right], \tag{11}$$

where the operation $\mathrm{vec}(\cdot)$ represents vectorization. Let $\dot{\mathbf{U}}$ be of rank R, and let the r-th eigenvalue and the corresponding eigenvector of $\dot{\mathbf{U}}$ be denoted by κ_r and $\mathbf{u}_r$, respectively. Then, (10) can be equivalently rewritten as

$$\mathbb{E}_{\eta_0}[\mathrm{J}(\mathbf{y};\eta_0)] = 2p_0\sum_{r=1}^{R}\kappa_r\left(\mathbf{U}_r\mathbf{x}\right)^{\mathsf{H}}\mathbf{\Sigma}_0^{-1}(\mathbf{x})\left(\mathbf{U}_r\mathbf{x}\right), \tag{12}$$

where $\mathbf{U}_r = \mathrm{vec}^{-1}(\mathbf{u}_r)$ and $\kappa_r \ge 0$.

Proof: Since $\mathbf{\Sigma}_0$ is positive definite, we can decompose its inverse as $\mathbf{\Sigma}_0^{-1} = \mathbf{V}^{\mathsf{H}}\mathbf{V}$. Based on the properties of the Kronecker product, denoted here as $\otimes$, (6) can be rewritten as follows:

$$\begin{aligned} \mathrm{J}\left(\mathbf{y};\eta_0\right) &= 2p_0 \left[\left(\mathbf{x}^{\mathsf{T}}\otimes\mathbf{V}\right)\mathrm{vec}(\dot{\mathbf{H}}_0)\right]^{\mathsf{H}}\left[\left(\mathbf{x}^{\mathsf{T}}\otimes\mathbf{V}\right)\mathrm{vec}(\dot{\mathbf{H}}_0)\right] \\ &= 2p_0\,\mathrm{vec}^{\mathsf{H}}(\dot{\mathbf{H}}_0)\left[\mathbf{x}^*\mathbf{x}^{\mathsf{T}}\otimes\mathbf{V}^{\mathsf{H}}\mathbf{V}\right]\mathrm{vec}(\dot{\mathbf{H}}_0) \\ &= 2p_0\,\mathrm{Tr}\left(\left(\mathbf{x}^*\mathbf{x}^{\mathsf{T}}\otimes\mathbf{\Sigma}_0^{-1}\right)\left(\mathrm{vec}(\dot{\mathbf{H}}_0)\mathrm{vec}^{\mathsf{H}}(\dot{\mathbf{H}}_0)\right)\right). \end{aligned} \tag{13}$$

Then, the expectation in (10) can be equivalently rewritten as

$$\mathbb{E}_{\eta_0}[\mathrm{J}\left(\mathbf{y};\eta_0\right)] = 2p_0\,\mathrm{Tr}\left(\left(\mathbf{x}^*\mathbf{x}^{\mathsf{T}}\otimes\mathbf{\Sigma}_0^{-1}\right)\dot{\mathbf{U}}\right), \tag{14}$$

where $\dot{\mathbf{U}}$ is the expectation given in (11). Since $\dot{\mathbf{U}}$ is a positive semi-definite matrix, it has an eigenvalue decomposition as

$$\dot{\mathbf{U}} = \sum_{r=1}^{R}\kappa_r\mathbf{u}_r\mathbf{u}_r^{\mathsf{H}}, \tag{15}$$

where κ_r and $\mathbf{u}_r$ are the r-th eigenvalue and the corresponding eigenvector of $\dot{\mathbf{U}}$, respectively. Then, substituting (15) into (14) and reversing the derivation of (13) give us (12). ■

Remark 1: The classic CRLB is a special case of the above, where η_0 is deterministic and the prior distribution $p(\eta_0)$ has zero variance. In this case, the rank of $\dot{\mathbf{U}}$ is one, and (12) reduces to (6).

B. Communication Performance Metric

For the communication users, we denote the uplink receive combining matrix as $\mathbf{W}$ with the column $\mathbf{w}_k$ as the beamformer for the k-th communication user, where $\|\mathbf{w}_k\|_2^2 = 1$. The SINR of the k-th communication user is

$$\gamma_k = \frac{p_k\left|\mathbf{w}_k^{\mathsf{H}}\left(\mathbf{H}_k\mathbf{x}\right)\right|^2}{\sum\limits_{k'\neq 0,k} p_{k'}\left|\mathbf{w}_k^{\mathsf{H}}\left(\mathbf{H}_{k'}\mathbf{x}\right)\right|^2 + p_0\,\mathbb{E}_{\eta_0}\left[\left|\mathbf{w}_k^{\mathsf{H}}\left(\mathbf{H}_0\mathbf{x}\right)\right|^2\right] + \sigma^2}. \tag{16}$$

For a fixed RIS beamforming vector $\mathbf{x}$, optimizing the receive combining vector $\mathbf{w}_k$ to maximize the SINR γ_k is a generalized Rayleigh quotient problem

$$\underset{\mathbf{w}_k}{\mathrm{maximize}}\quad \gamma_k = \frac{p_k\mathbf{w}_k^{\mathsf{H}}\left(\mathbf{H}_k\mathbf{x}\right)\left(\mathbf{H}_k\mathbf{x}\right)^{\mathsf{H}}\mathbf{w}_k}{\mathbf{w}_k^{\mathsf{H}}\mathbf{\Sigma}_k(\mathbf{x})\mathbf{w}_k}, \tag{17}$$

where the covariance matrix $\mathbf{\Sigma}_k(\mathbf{x})$ is given by

$$\begin{aligned} \mathbf{\Sigma}_k(\mathbf{x}) = &\sum_{k'\neq 0,\, k'\neq k} p_{k'}\left(\mathbf{H}_{k'}\mathbf{x}\right)\left(\mathbf{H}_{k'}\mathbf{x}\right)^{\mathsf{H}} \\ &+ p_0\,\mathbb{E}_{\eta_0}\left[\left(\mathbf{H}_0\mathbf{x}\right)\left(\mathbf{H}_0\mathbf{x}\right)^{\mathsf{H}}\right] + \sigma^2\mathbf{I}. \end{aligned} \tag{18}$$

The expectation in (18) can be expressed as

$$\mathbb{E}_{\eta_0}\left[\left(\mathbf{H}_0\mathbf{x}\right)\left(\mathbf{H}_0\mathbf{x}\right)^{\mathsf{H}}\right] = \mathrm{vec}^{-1}\left(\mathbb{E}_{\eta_0}[\mathbf{H}_0^*\otimes\mathbf{H}_0]\,\mathrm{vec}\left(\mathbf{x}\mathbf{x}^{\mathsf{H}}\right)\right), \tag{19}$$

so that $\mathbf{x}$ can be separated from the expectation. The optimal solution $\mathbf{w}_k^\star$ is a function of $\mathbf{x}$ and can be found in closed-form:

$$\mathbf{w}_k^\star = \left[\mathbf{\Sigma}_k^{-1}(\mathbf{x})\,\mathbf{H}_k\mathbf{x}\right] / \left\|\mathbf{\Sigma}_k^{-1}(\mathbf{x})\,\mathbf{H}_k\mathbf{x}\right\|, \tag{20}$$

With this optimal receive combining vector $\mathbf{w}_k^\star$, the SINR (16) can be rewritten as follows:

$$\gamma_k(\mathbf{x}) = p_k\left(\mathbf{H}_k\mathbf{x}\right)^{\mathsf{H}}\mathbf{\Sigma}_k^{-1}(\mathbf{x})\left(\mathbf{H}_k\mathbf{x}\right). \tag{21}$$

C. Problem Formulation

We now formulate the overall joint sensing and communication problem as that of minimizing the BCRLB while ensuring SINR constraints for the communication users. For the case where the RIS is active, (2) is the amplitude constraint. Then, the optimization problem is formulated as

$$\begin{aligned} (\mathrm{P1}):\quad &\underset{\mathbf{x}}{\mathrm{maximize}}\quad \mathbb{E}_{\eta_0}[\mathrm{J}\left(\mathbf{y};\eta_0\right)] && \text{(22a)}\\ &\text{subject to}\quad \gamma_k(\mathbf{x})\geq\Gamma,\quad \forall k\neq 0, && \text{(22b)}\\ &\qquad\qquad\quad |x_n|\leq\alpha_{\max},\quad \forall n, && \text{(22c)} \end{aligned}$$

where Γ is the given SINR threshold. For the case where the RIS is passive, the amplitude constraint is (3), and the optimization problem is formulated as

$$\begin{aligned} (\mathrm{P1}^*):\quad &\underset{\mathbf{x}}{\mathrm{maximize}}\quad \mathbb{E}_{\eta_0}[\mathrm{J}\left(\mathbf{y};\eta_0\right)] && \text{(23a)}\\ &\text{subject to}\quad \gamma_k(\mathbf{x})\geq\Gamma,\quad \forall k\neq 0, && \text{(23b)}\\ &\qquad\qquad\quad |x_n| = 1,\qquad \forall n. && \text{(23c)} \end{aligned}$$

The choice of SINR threshold affects the trade-off between sensing and communications. When $\Gamma = 0$, the problem reduces to the sensing-only problem. The main observation of this paper is that the formulated problems are FCFP. Specifically, they have sum-of-ratios as the objective function (i.e., (12)) and fractional constraints (i.e., (21)).

IV. Joint Sensing and Communications

We first consider (P1) since its RIS amplitude constraint is convex and is easier to handle, then proceed to (P1*).

A. Quadratic Transform-Based FCFP for (P1)

In problem (P1), both the objective function and the SINR constraints contain fractional structures. To tackle such a highly nontrivial FCFP, we first rewrite problem (P1) as

$$\begin{aligned} &\underset{\mathbf{x}}{\mathrm{maximize}}\quad \sum_{r=1}^{R}\kappa_r\left(\mathbf{U}_r\mathbf{x}\right)^{\mathsf{H}}\mathbf{\Sigma}_0^{-1}(\mathbf{x})\left(\mathbf{U}_r\mathbf{x}\right) && \text{(24a)}\\ &\text{subject to}\quad \left(\mathbf{H}_k\mathbf{x}\right)^{\mathsf{H}}\mathbf{\Sigma}_k^{-1}(\mathbf{x})\left(\mathbf{H}_k\mathbf{x}\right)\geq\Gamma_k,\ \ \forall k\neq 0, && \text{(24b)}\\ &\qquad\qquad\quad |x_n|\leq\alpha_{\max},\ \ \forall n, && \text{(24c)} \end{aligned}$$

where $\Gamma_k = \Gamma/p_k$.

The main idea is to apply a quadratic transform technique to this problem. Quadratic transform is originally proposed for fractional programming problems with fractional structure in the objective function only [13]. The main result of this paper is that it can also be applied when there are fractional structures both in the objective and the constraints.

Theorem 2: For a maximization problem with fractional structures in both objective function and constraints as

$$\begin{aligned} &\underset{\mathbf{x}}{\mathrm{maximize}}\quad \sum_{k\in\mathcal{S}}\mathbf{a}_k^{\mathsf{H}}(\mathbf{x})\,\mathbf{B}_k^{-1}(\mathbf{x})\,\mathbf{a}_k(\mathbf{x}) && \text{(25a)}\\ &\text{subject to}\quad \mathbf{a}_k^{\mathsf{H}}(\mathbf{x})\,\mathbf{B}_k^{-1}(\mathbf{x})\,\mathbf{a}_k(\mathbf{x})\geq\Gamma_k,\quad \forall k\notin\mathcal{S}, && \text{(25b)} \end{aligned}$$

where $\mathbf{B}_k(\mathbf{x})$ is Hermitian and positive definite, it is equivalent to the following problem:

$$\underset{\mathbf{x},\boldsymbol{\lambda}_k}{\text{minimize}} \quad \sum_{k\in\mathcal{S}} f_k\left(\mathbf{x},\boldsymbol{\lambda}_k\right) \tag{26a}$$

$$\text{subject to} \quad f_k\left(\mathbf{x},\boldsymbol{\lambda}_k\right)+\Gamma_k\le 0, \quad \forall k\notin\mathcal{S}, \tag{26b}$$

where

$$f_k\left(\mathbf{x},\boldsymbol{\lambda}_k\right)=\boldsymbol{\lambda}_k^{\mathsf{H}}\mathbf{B}_k(\mathbf{x})\,\boldsymbol{\lambda}_k-2\,\mathrm{Re}\left\{\boldsymbol{\lambda}_k^{\mathsf{H}}\mathbf{a}_k(\mathbf{x})\right\}. \tag{27}$$

Here, $\boldsymbol{\lambda}_k$ is the auxiliary variable introduced to decouple the numerator and denominator of a fractional structure.

Proof: The key is to recognize the following relationship, which can be verified by expanding the terms:

$$\begin{aligned}
&\boldsymbol{\lambda}_k^{\mathsf{H}}\mathbf{B}_k(\mathbf{x})\,\boldsymbol{\lambda}_k-2\,\mathrm{Re}\left\{\boldsymbol{\lambda}_k^{\mathsf{H}}\mathbf{a}_k(\mathbf{x})\right\}\\
&=\left[\boldsymbol{\lambda}_k-\mathbf{B}_k^{-1}(\mathbf{x})\,\mathbf{a}_k(\mathbf{x})\right]^{\mathsf{H}}\mathbf{B}_k(\mathbf{x})\left[\boldsymbol{\lambda}_k-\mathbf{B}_k^{-1}(\mathbf{x})\,\mathbf{a}_k(\mathbf{x})\right]\\
&\quad-\mathbf{a}_k^{\mathsf{H}}(\mathbf{x})\,\mathbf{B}_k^{-1}(\mathbf{x})\,\mathbf{a}_k(\mathbf{x})\,.
\end{aligned} \tag{28}$$

Observe that the above expression is minimized when the auxiliary variable is chosen as follows:

$$\boldsymbol{\lambda}_k^{\star}=\mathbf{B}_k^{-1}(\mathbf{x})\,\mathbf{a}_k(\mathbf{x})\,, \tag{29}$$

in which case

$$\boldsymbol{\lambda}_k^{\star\mathsf{H}}\mathbf{B}_k(\mathbf{x})\,\boldsymbol{\lambda}_k^{\star}-2\,\mathrm{Re}\left\{\boldsymbol{\lambda}_k^{\star\mathsf{H}}\mathbf{a}_k(\mathbf{x})\right\}=-\,\mathbf{a}_k^{\mathsf{H}}(\mathbf{x})\,\mathbf{B}_k^{-1}(\mathbf{x})\,\mathbf{a}_k(\mathbf{x})\,. \tag{30}$$

Now consider the optimization problem (26) as an outer minimization over $\mathbf{x}$ together with an inner minimization over $\boldsymbol{\lambda}_k$. For fixed $\mathbf{x}$, the objective of the inner problem is minimized when $\boldsymbol{\lambda}_k^{\star}=\mathbf{B}_k^{-1}\mathbf{a}_k(\mathbf{x})$ for all $k\in\mathcal{S}$.

For the constraints, each choice of $\boldsymbol{\lambda}_k$ in the inner problem gives rise to a different constraint set over $\mathbf{x}$ for the outer problem. But it can be seen that the choice of $\boldsymbol{\lambda}_k^{\star}=\mathbf{B}_k^{-1}\mathbf{a}_k(\mathbf{x})$ makes the resulting constraint sets the *largest*. Thus, to help the outer optimization achieve its minimum, we should set $\boldsymbol{\lambda}_k^{\star}=\mathbf{B}_k^{-1}\mathbf{a}_k(\mathbf{x})$ for all $k\notin\mathcal{S}$.

Together, the above choices of $\boldsymbol{\lambda}_k^{\star}$ make (30) to hold. In this case, the outer optimization over $\mathbf{x}$ in (26) and the optimization (25) are identical, because both the objective function and the constraints are the same. Therefore, (26) is equivalent to (25). ■

Based on Theorem 2, the problem (24) can be equivalently transformed into the following problem:

$$\underset{\mathbf{x},\boldsymbol{\lambda}_r,\boldsymbol{\lambda}_k}{\text{minimize}} \quad \sum_{r=1}^{R}\kappa_r f_r\left(\mathbf{x},\boldsymbol{\lambda}_r\right) \tag{31a}$$

$$\text{subject to} \quad f_k\left(\mathbf{x},\boldsymbol{\lambda}_k\right)+\Gamma_k\le 0, \quad \forall k\neq 0, \tag{31b}$$

$$|x_n|\le\alpha_{\max}, \quad \forall n, \tag{31c}$$

where the new transformed functions are given by

$$f_r\left(\mathbf{x},\boldsymbol{\lambda}_r\right)=\boldsymbol{\lambda}_r^{\mathsf{H}}\boldsymbol{\Sigma}_0(\mathbf{x})\,\boldsymbol{\lambda}_r-2\,\mathrm{Re}\left\{\boldsymbol{\lambda}_r^{\mathsf{H}}\mathbf{U}_r\mathbf{x}\right\}, \tag{32}$$

$$f_k\left(\mathbf{x},\boldsymbol{\lambda}_k\right)=\boldsymbol{\lambda}_k^{\mathsf{H}}\boldsymbol{\Sigma}_k(\mathbf{x})\,\boldsymbol{\lambda}_k-2\,\mathrm{Re}\left\{\boldsymbol{\lambda}_k^{\mathsf{H}}\mathbf{H}_k\mathbf{x}\right\}. \tag{33}$$

This problem can now be solved numerically by iteratively optimizing the auxiliary variables and the passive RIS beamforming vector to reach a stationary point.

When $\mathbf{x}$ is held fixed, the optimal $\boldsymbol{\lambda}_r^{\star}$ and $\boldsymbol{\lambda}_k^{\star}$ can be easily found in closed form as in (29):

$$\boldsymbol{\lambda}_r^{\star}=\boldsymbol{\Sigma}_0^{-1}(\mathbf{x})\,\mathbf{U}_r\mathbf{x}, \quad \forall r, \tag{34}$$

$$\boldsymbol{\lambda}_k^{\star}=\boldsymbol{\Sigma}_k^{-1}(\mathbf{x})\,\mathbf{H}_k\mathbf{x}, \quad \forall k\neq 0. \tag{35}$$

It is interesting to observe that the optimal auxiliary variables $\boldsymbol{\lambda}_k^{\star}$ are equal to the optimal receive combining vectors,

$$\frac{\boldsymbol{\lambda}_k^{\star}}{\|\boldsymbol{\lambda}_k^{\star}\|}=\frac{\boldsymbol{\Sigma}_k^{-1}(\mathbf{x})\,\mathbf{H}_k\mathbf{x}}{\|\boldsymbol{\Sigma}_k^{-1}(\mathbf{x})\,\mathbf{H}_k\mathbf{x}\|}=\mathbf{w}_k^{\star}, \quad \forall k\neq 0. \tag{36}$$

When the auxiliary variables $\boldsymbol{\lambda}_r^{\star}$ and $\boldsymbol{\lambda}_k^{\star}$ are held fixed, the second term in (32) is affine. For the first term in (32), it can be rewritten as

$$\begin{aligned}
\boldsymbol{\lambda}_r^{\star\mathsf{H}}\boldsymbol{\Sigma}_0(\mathbf{x})\boldsymbol{\lambda}_r^{\star}&=\boldsymbol{\lambda}_r^{\star\mathsf{H}}\left(\sum_{k\neq 0}p_k\left(\mathbf{H}_k\mathbf{x}\right)\left(\mathbf{H}_k\mathbf{x}\right)^{\mathsf{H}}+\sigma^2\mathbf{I}\right)\boldsymbol{\lambda}_r^{\star}\\
&=\mathbf{x}^{\mathsf{H}}\left(\sum_{k\neq 0}p_k(\mathbf{H}_k^{\mathsf{H}}\boldsymbol{\lambda}_r^{\star})(\mathbf{H}_k^{\mathsf{H}}\boldsymbol{\lambda}_r^{\star})^{\mathsf{H}}\right)\mathbf{x}+\sigma^2\left\|\boldsymbol{\lambda}_r^{\star}\right\|^2\\
&\triangleq\mathbf{x}^{\mathsf{H}}\boldsymbol{\Upsilon}_r\mathbf{x}+\sigma^2\left\|\boldsymbol{\lambda}_r^{\star}\right\|^2,
\end{aligned} \tag{37}$$

where $\boldsymbol{\Upsilon}_r$ is positive semi-definite. Consequently, the function in (32) is convex with respect to $\mathbf{x}$,

$$f_r\left(\mathbf{x},\boldsymbol{\lambda}_r^{\star}\right)=\mathbf{x}^{\mathsf{H}}\boldsymbol{\Upsilon}_r\mathbf{x}-2\,\mathrm{Re}\left\{\boldsymbol{\lambda}_r^{\star\mathsf{H}}\mathbf{U}_r\mathbf{x}\right\}+\sigma^2\left\|\boldsymbol{\lambda}_r^{\star}\right\|^2. \tag{38}$$

Similarly, the function in (33) can be rewritten in the following convex form,

$$f_k\left(\mathbf{x},\boldsymbol{\lambda}_k^{\star}\right)=\mathbf{x}^{\mathsf{H}}\boldsymbol{\Upsilon}_k\mathbf{x}-2\,\mathrm{Re}\left\{\boldsymbol{\lambda}_k^{\star\mathsf{H}}\mathbf{H}_k\mathbf{x}\right\}+\sigma^2\left\|\boldsymbol{\lambda}_k^{\star}\right\|^2, \tag{39}$$

where the positive semi-definite matrix $\boldsymbol{\Upsilon}_k$ is given by

$$\begin{aligned}
\boldsymbol{\Upsilon}_k=&\sum_{k'\neq 0,\ k'\neq k}p_{k'}\left(\mathbf{H}_{k'}^{\mathsf{H}}\boldsymbol{\lambda}_k^{\star}\right)\left(\mathbf{H}_{k'}^{\mathsf{H}}\boldsymbol{\lambda}_k^{\star}\right)^{\mathsf{H}}\\
&+p_0\,\mathbb{E}_{\eta_0}\left[\left(\mathbf{H}_0^{\mathsf{H}}\boldsymbol{\lambda}_k^{\star}\right)\left(\mathbf{H}_0^{\mathsf{H}}\boldsymbol{\lambda}_k^{\star}\right)^{\mathsf{H}}\right].
\end{aligned} \tag{40}$$

The expectation in (40) can be computed by

$$\begin{aligned}
&\mathbb{E}_{\eta_0}\left[\left(\mathbf{H}_0^{\mathsf{H}}\boldsymbol{\lambda}_k^{\star}\right)\left(\mathbf{H}_0^{\mathsf{H}}\boldsymbol{\lambda}_k^{\star}\right)^{\mathsf{H}}\right]\\
&\quad=\mathrm{vec}^{-1}\Big(\mathbb{E}_{\eta_0}\left(\mathbf{H}_0^{\mathsf{T}}\otimes\mathbf{H}_0^{\mathsf{H}}\right)\mathrm{vec}\Big(\boldsymbol{\lambda}_k^{\star}\boldsymbol{\lambda}_k^{\star\mathsf{H}}\Big)\Big),
\end{aligned} \tag{41}$$

so that there is no need to recompute the expectation each time $\boldsymbol{\lambda}_k^{\star}$ is updated. Then, the sub-problem of optimizing $\mathbf{x}$ can be formulated as

$$(\text{P2}):\quad \underset{\mathbf{x}}{\text{minimize}} \quad \sum_{r=1}^{R}\kappa_r f_r\left(\mathbf{x},\boldsymbol{\lambda}_r^{\star}\right) \tag{42a}$$

$$\text{subject to} \quad f_k\left(\mathbf{x},\boldsymbol{\lambda}_k^{\star}\right)+\Gamma_k\le 0, \quad \forall k\neq 0, \tag{42b}$$

$$|x_n|\le\alpha_{\max}, \quad \forall\, n. \tag{42c}$$

The above sub-problem is a convex quadratically constrained quadratic program (QCQP), and the optimal solution can be easily obtained by an optimization solver such as the CVX.

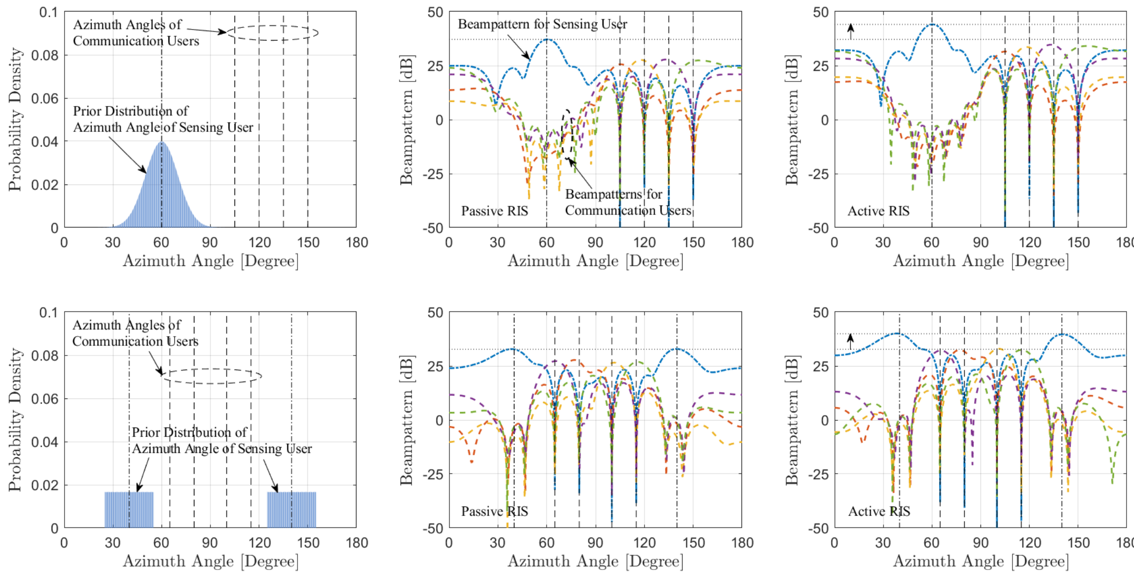

Fig. 2. Reflecting beampatterns with different prior distributions of the azimuth angle of sensing user and different directions of communication users.

B. Penalty Quadratic Transform-Based FCFP for (P1)*

Now, consider the case of passive RIS. Similar to problem (P1), Theorem 2 can also be applied to problem (P1*). Then, the equivalently transformed problem of (P1*) is

$$\underset{\mathbf{x},\boldsymbol{\lambda}_r,\boldsymbol{\lambda}_k}{\text{minimize}} \quad \sum_{r=1}^{R} \kappa_r f_r\left(\mathbf{x}, \boldsymbol{\lambda}_r\right) \tag{43a}$$

$$\text{subject to} \quad f_k\left(\mathbf{x}, \boldsymbol{\lambda}_k\right) + \Gamma_k \leq 0, \quad \forall k \neq 0, \tag{43b}$$

$$|x_n| = 1, \quad \forall n, \tag{43c}$$

The only difference from the active case is that the amplitude constraints of the RIS are now unit-modulus, which are non-convex and not easy to address. To handle the unit-modulus constraints, we directly include a penalty term into the objective function. Then, the problem (43) is reformulated as

$$\underset{\mathbf{x},\boldsymbol{\theta},\boldsymbol{\lambda}_r,\boldsymbol{\lambda}_k}{\text{minimize}} \quad \sum_{r=1}^{R} \kappa_r f_r\left(\mathbf{x}, \boldsymbol{\lambda}_r\right) + \mu \left\|\mathbf{x} - \boldsymbol{\theta}\right\|^2 \tag{44a}$$

$$\text{subject to} \quad f_k\left(\mathbf{x}, \boldsymbol{\lambda}_k\right) + \Gamma_k \leq 0, \quad \forall k \neq 0, \tag{44b}$$

where μ determines the extent of penalty, and $\boldsymbol{\theta}$ is defined as

$$\boldsymbol{\theta}^{\mathsf{T}} = \left[\exp\left(j\theta_1\right), \exp\left(j\theta_2\right), \cdots, \exp\left(j\theta_{N^2}\right)\right]. \tag{45}$$

This problem can be solved by iteratively updating the auxiliary variables $\boldsymbol{\theta}$, $\boldsymbol{\lambda}_r$, $\boldsymbol{\lambda}_k$, and the optimization variable $\mathbf{x}$.

When $\mathbf{x}$ is fixed, the optimal $\boldsymbol{\lambda}_r^\star$ and $\boldsymbol{\lambda}_k^\star$ are the same as that in (34) and (35), respectively. The optimal $\boldsymbol{\theta}^\star$ can be obtained by solving the following problem:

$$\underset{-\pi \leq \theta_n \leq \pi}{\text{minimize}} \quad \sum_{n=1}^{N^2} \left|x_n - e^{j\theta_n}\right|^2. \tag{46}$$

Since the optimization variables θ_n's are separable in (46), the optimal θ_n is simply $\arg(x_n)$.

When $\boldsymbol{\theta}^\star$, $\boldsymbol{\lambda}_r^\star$, and $\boldsymbol{\lambda}_k^\star$ are held fixed, the sub-problem of updating $\mathbf{x}$ can be formulated as

$$(\text{P2*}): \quad \underset{\mathbf{x}}{\text{minimize}} \quad \sum_{r=1}^{R} \kappa_r f_r\left(\mathbf{x}, \boldsymbol{\lambda}_r^\star\right) + \mu \left\|\mathbf{x} - \boldsymbol{\theta}^\star\right\|^2 \tag{47a}$$

$$\text{such that} \quad f_k\left(\mathbf{x}, \boldsymbol{\lambda}_k^\star\right) + \Gamma_k \leq 0, \quad \forall k \neq 0, \tag{47b}$$

which is also a convex QCQP similar to problem (P2). Note that the penalty coefficient μ can be updated using $\mu = \alpha\mu$ with a suitable factor α along each iteration to balance between accuracy and convergence.

V. Numerical Results

In this section, we provide numerical results to show the effectiveness of the proposed algorithms in various scenarios. The simulation environment is as follows. The BS is equipped with $M = 16$ antennas. For both the sensing user and communication users, we set their transmit powers such that p_k/σ^2 is -5 dB (unless otherwise specified). The SINR threshold for the communication users is set to 15 dB. The number of reflecting elements is set to 10×10. For the active RIS, the maximum amplification gain is $a_{\max}^2 = 5$ dB.

We consider two scenarios: (i) four communication users at $105°$, $120°$, $135°$, and $150°$, respectively, and one sensing user, whose azimuth angle has a prior distribution centered at $60°$, as shown in the top row of Fig. 2; (ii) four communication users at $65°$, $80°$, $100°$, and $115°$, respectively, and one sensing user, whose azimuth angle has a prior distribution which is a uniform distribution over the ranges $[25°, 55°]$ and $[125°, 155°]$, as shown in the bottom row of Fig. 2. The designed RIS beampatterns of passive cases are shown in the second column and those of active cases are shown in the third column. The RIS beampattern for the k-th user is defined as

$$\mathcal{Q}_k = \left|\mathbf{w}_k^{\mathsf{H}} \left[\mathbf{G}\boldsymbol{\Phi}\mathbf{v}(\eta)\right]\right|^2, \tag{48}$$

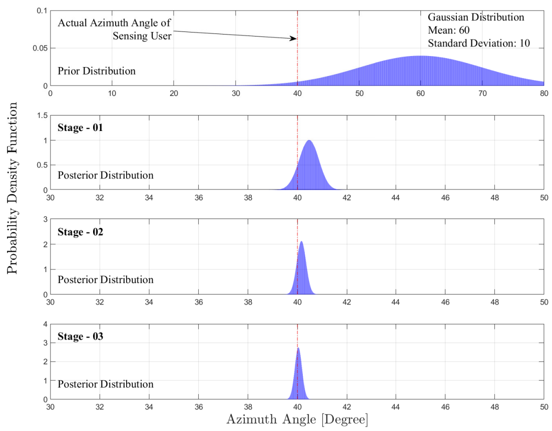

Fig. 3. Posterior distributions over three iterations with adaptive RIS sensing.

which is the received signal power after linear minimum mean square error (LMMSE) combining at the BS from a unit-power transmitter at an azimuth angle η with respect to the RIS. As comparison, we also plot the received signal power for the sensing user, if utilizing a linear combiner $\mathbf{w}_0$ similar for the communication users as given below:

$$\mathbf{w}_0 = \boldsymbol{\delta}_{\max}\left(\boldsymbol{\Sigma}_0^{-1}(\mathbf{x})\,\mathbb{E}_{\eta_0}\left[\left(\dot{\mathbf{H}}_0\mathbf{x}\right)\left(\dot{\mathbf{H}}_0\mathbf{x}\right)^{\mathsf{H}}\right]\right), \tag{49}$$

where $\boldsymbol{\delta}_{\max}(\mathbf{A})$ denotes the eigenvector corresponding to the largest eigenvalue of $\mathbf{A}$.

The designed RIS beamforming patterns are interpretable. From Fig. 2, it can be observed that the solutions of the optimization problem produce beams that are aligned with the directions of communication users, while also having a peak matching the prior distribution of the sensing angle. Moreover, compared to the passive RIS, the active RIS can provide better sensing performance while meeting communication requirements. This improvement is attributed not only to the additional power but also to additional degrees of freedom available for beamforming for the active RIS.

To further illustrate the sensing performance of the proposed algorithm, we show evolution of the posterior distributions after several iterations of sensing stages in Fig. 3. The posterior probability function of the $(t+1)$-th sensing stage is computed as follows. Note that the communication signals are regarded as noise for sensing. In this case, we have

$$\begin{aligned}\mathcal{P}(\eta_0 \,|\, \mathbf{y}_{t+1}) &\propto \mathcal{L}(\mathbf{y}_{t+1} \,|\, \eta_0)\cdot\mathcal{P}(\eta_0 \,|\, \mathbf{y}_t) \\ &= \mathcal{CN}(s_0\mathbf{H}_0\mathbf{x}, \boldsymbol{\Sigma}_0(\mathbf{x}))\cdot\mathcal{P}(\eta_0 \,|\, \mathbf{y}_t),\end{aligned} \tag{50}$$

where $\mathcal{L}(\mathbf{y}_{t+1} \,|\, \eta_0)$ is the likelihood function of the received signal $\mathbf{y}_{t+1}$, and $\mathcal{P}(\eta_0 \,|\, \mathbf{y}_t)$ is the posterior distribution from the previous iteration, which is used as the prior distribution $p(\eta_0)$ for the current iteration. We show the result for the passive RIS case in the first scenario in Fig. 2. The true angle of the sensing user is at 40°. The communication signals are randomly generated from a Gaussian distribution. The pilot signal for the sensing user is a known sequence with $p_0/\sigma^2 = -20$ dB. In Fig. 3, we plot the posterior distribution of η_0 after three iterations using the RIS beamforming vector designed by the proposed algorithm. From Fig. 3, we can see that as the number of sensing stages increases, the posterior distribution rapidly converges to a highly concentrated distribution with a peak at the true sensing angle. This shows that the proposed beamforming design is highly effective for sensing.

VI. Conclusion

This paper proposes a methodology for RIS beamforming pattern design for an uplink RIS-assisted integrated sensing and communications scenario. We formulate the optimization problem of minimizing the BCRLB of azimuth angle estimation for the sensing user, while imposing SINR constraints for multiple communication users. This problem is a non-convex fractional program with fractional constraints. We extend a quadratic transform technique to handle the fractional structures in both the objective function and the constraints, then transform the problem into a sequence of convex QCQP. Simulation results demonstrate highly effective RIS beampattern design for both sensing and communications.

References

[1] F. Liu, Y. Cui, C. Masouros, J. Xu, T. X. Han, Y. C. Eldar, and S. Buzzi, “Integrated sensing and communications: Toward dual-functional wireless networks for 6G and beyond,” *IEEE J. Sel. Areas Commun.*, vol. 40, no. 6, pp. 1728–1767, Jun. 2022.

[2] Q. Wu and R. Zhang, “Intelligent reflecting surface enhanced wireless network via joint active and passive beamforming,” *IEEE Trans. Wireless Commun.*, vol. 18, no. 11, pp. 5394–5409, Nov. 2019.

[3] R. Long, Y.-C. Liang, Y. Pei, and E. G. Larsson, “Active reconfigurable intelligent surface-aided wireless communications,” *IEEE Trans. Wireless Commun.*, vol. 20, no. 8, pp. 4962–4975, Aug. 2021.

[4] Z.-M. Jiang, M. Rihan, P. Zhang, L. Huang, Q. Deng, J. Zhang, and E. M. Mohamed, “Intelligent reflecting surface aided dual-function radar and communication system,” *IEEE Syst. J.*, vol. 16, no. 1, pp. 475–486, Mar. 2022.

[5] R. Liu, M. Li, Y. Liu, Q. Wu, and Q. Liu, “Joint transmit waveform and passive beamforming design for RIS-aided DFRC systems,” *IEEE J. Sel. Topics Signal Process.*, vol. 16, no. 5, pp. 995–1010, Aug. 2022.

[6] X. Shao, C. You, W. Ma, X. Chen, and R. Zhang, “Target sensing with intelligent reflecting surface: Architecture and performance,” *IEEE J. Sel. Areas Commun.*, vol. 40, no. 7, pp. 2070–2084, Jul. 2022.

[7] E. Grossi, H. Taremizadeh, and L. Venturino, “Radar target detection and localization aided by an active reconfigurable intelligent surface,” *IEEE Signal Process. Lett.*, vol. 30, pp. 903–907, 2023.

[8] S. Buzzi, E. Grossi, M. Lops, and L. Venturino, “Foundations of MIMO radar detection aided by reconfigurable intelligent surfaces,” *IEEE Trans. Signal Process.*, vol. 70, pp. 1749–1763, 2022.

[9] Y. Liu, E. Liu, R. Wang, and Y. Geng, “Reconfigurable intelligent surface aided wireless localization,” in *Prof. IEEE Int. Conf. Commun.*, Montreal, Canada, Jun. 2021, pp. 1–6.

[10] F. Liu, Y.-F. Liu, A. Li, C. Masouros, and Y. C. Eldar, “Cramér-rao bound optimization for joint radar-communication beamforming,” *IEEE Trans. Signal Process.*, vol. 70, pp. 240–253, 2022.

[11] X. Song, J. Xu, F. Liu, T. X. Han, and Y. C. Eldar, “Intelligent reflecting surface enabled sensing: Cramér-rao bound optimization,” *IEEE Trans. Signal Process.*, vol. 71, pp. 2011–2026, 2023.

[12] W. Huleihel, J. Tabrikian, and R. Shavit, “Optimal adaptive waveform design for cognitive mimo radar,” *IEEE Trans. Signal Processing*, vol. 61, no. 20, pp. 5075–5089, 2013.

[13] K. Shen and W. Yu, “Fractional programming for communication systems—Part I: Power control and beamforming,” *IEEE Trans. Signal Process.*, vol. 66, no. 10, May 2018.

[14] Q. Wu, S. Zhang, B. Zheng, C. You, and R. Zhang, “Intelligent reflecting surface-aided wireless communications: A tutorial,” *IEEE Trans. Commun.*, vol. 69, no. 5, pp. 3313–3351, May 2021.

[15] F. Sohrabi, Z. Chen, and W. Yu, “Deep active learning approach to adaptive beamforming for mmwave initial alignment,” *IEEE J. Sel. Areas Commun.*, vol. 39, no. 8, pp. 2347–2360, 2021.